



A fractal Richards' equation to capture the non-Boltzmann scaling of water transport in unsaturated media



HongGuang Sun^{a,e,*}, Mark M. Meerschaert^b, Yong Zhang^{c,*}, Jianting Zhu^d, Wen Chen^{a,e,*}

^a State Key Laboratory of Hydrology-Water Resources and Hydraulic Engineering, College of Mechanics and Materials, Hohai University, Nanjing 210098, China

^b Department of Statistics and Probability, Michigan State University, East Lansing, MI 48824, United States

^c Division of Hydrologic Sciences, Desert Research Institute, Las Vegas, NV 89119, United States

^d Department of Civil and Architectural Engineering, University of Wyoming 1000 E. University Ave Laramie, WY 82071, United States

^e Institute of Soft Matter Mechanics, Department of Engineering Mechanics, Hohai University, Nanjing 210098, China

ARTICLE INFO

Article history:

Received 5 July 2012

Received in revised form 6 November 2012

Accepted 7 November 2012

Available online 5 December 2012

Keywords:

Richards' equation
Non-Boltzmann scaling
Fractal model
Water content

ABSTRACT

The traditional Richards' equation implies that the wetting front in unsaturated soil follows Boltzmann scaling, with travel distance growing as the square root of time. This study proposes a fractal Richards' equation (FRE), replacing the integer-order time derivative of water content by a fractal derivative, using a power law ruler in time. FRE solutions exhibit anomalous non-Boltzmann scaling, attributed to the fractal nature of heterogeneous media. Several applications are presented, fitting the FRE to water content curves from previous literature.

© 2012 Elsevier Ltd. All rights reserved.

1. Introduction

Richards' equation [14] is the fundamental model for describing flow through unsaturated media. For water flow through one-dimensional horizontal (or sorption) soils, Richards' equation takes the form

$$\frac{\partial \theta}{\partial t} = \frac{\partial}{\partial x} \left[D(\theta) \frac{\partial \theta}{\partial x} \right], \quad (1)$$

where θ ($L^3 L^{-3}$) is the volumetric water content, $D(\theta)$ ($L^2 T^{-1}$) is the water diffusivity, x (L) is the distance from the inlet of the horizontal medium column, and t (T) denotes ordinary (clock) time. This distinction is emphasized here for clarity, since the model developed later in this paper involves a different clock. Substitute $x = \lambda t^{1/2}$ into Eq. (1) and use the chain rule to obtain an ordinary differential equation (ODE)

$$-\frac{\lambda}{2} \frac{\partial \theta}{\partial \lambda} = \frac{\partial}{\partial \lambda} \left[D(\theta) \frac{\partial \theta}{\partial \lambda} \right]. \quad (2)$$

The Boltzmann scaling $x = \lambda t^{1/2}$ makes travel distance grow as the square root of time.

In many laboratory experiments and field measurements, the evolution of a horizontal wetting front deviates significantly from Boltzmann scaling, e.g., see [12]. These studies often reflect anomalous Boltzmann scaling

$$x = \lambda(\theta) t^{\alpha/2}, \quad (3)$$

where the dimensionless exponent $0 < \alpha < 2$. Fig. 1(a) illustrates non-Boltzmann scaling in a laboratory experiment from Guerrini and Swartzendruber [7]. Additional examples of anomalous non-Boltzmann scaling are summarized in Table 1. The 95% confidence bounds for $\alpha/2$ listed for the data of El Abd and Milczarek [4] conclusively demonstrate non-Boltzmann scaling, since they exclude 0.5. The other data sources did not give confidence bands.

Several model extensions have been proposed to capture non-Boltzmann scaling. Guerrini and Swartzendruber [7] and El Abd and Milczarek [4] allow diffusivity D to vary as a function of both water content and time, i.e., $D = D(\theta, t)$ (see further discussion below). Pachepsky et al. [12] propose a time-fractional Richards' equation

$$\mathbb{D}_t^\alpha \theta = \frac{\partial^\alpha \theta}{\partial t^\alpha} = \frac{\partial}{\partial x} \left[D_x(\theta) \frac{\partial \theta}{\partial x} \right], \quad (4)$$

where $\mathbb{D}_t^\alpha \theta$ denotes a Riemann–Liouville fractional derivative [11, Eq. (2.17)] of order $0 < \alpha \leq 1$. Gerolymatou et al. [6] note that the fractional Richards' Eq. (4) cannot be transformed into an ODE as in (2), due to complications with the fractional product rule, and

* Corresponding authors.

E-mail addresses: sunhongguang08@gmail.com (H. Sun), Yong.Zhang@dri.edu (Y. Zhang), chenwen@hhu.edu.cn (W. Chen).

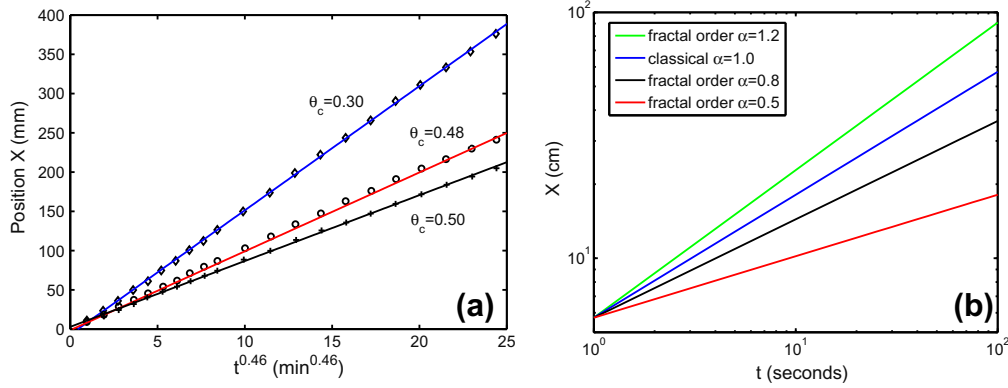


Fig. 1. (a) Relationship between the position of wetting front θ_c and the fractal time $t^{0.46}$ in infiltration experiments through horizontal soil columns by Guerrini and Swartzendruber [7]. (b) Isosaturation curves for volumetric water content $\theta = 0.2$ for different fractal derivative orders in the FRE (7) with $D_x = 10.0$. The order α of the fractal derivative corresponds to the slope in the double-log plot.

Table 1
Non-Boltzmann scaling observed in laboratory experiments and field measurements.

Data source	Medium	$\alpha/2$
El Abd and Milczarek [4]	White siliceous brick (sil #1)	0.430 ± 0.007
Ferguson and Gardner [5]	Salkum silty clay loam	0.455
Küntz and Lavallée [9]	A fired-clay brick	0.580
Küntz and Lavallée [9]	A Lépine limestone	0.610
El Abd and Milczarek [4]	Fired-clay brick (clay #1)	0.620 ± 0.010

modify the model (4) as a fractional integral equation. Küntz and Lavallée [9] and El Abd and Milczarek [4] use a modified Fick’s law $q = -D(\theta)(d\theta/dx)^n$ where n is a real number. This study proposes a simpler modification of Richards’ equation to capture non-Boltzmann scaling, using a fractal ruler in time. The new model exhibits non-Boltzmann scaling, and includes the super-diffusive case $\alpha > 1$. The model leads to an ODE using the non-Boltzmann scaling, and provides an improved fit to the experimental data of El Abd and Milczarek [4].

2. Fractal Richards’ equation

Soil heterogeneity can have a profound effect on unsaturated flow, disrupting Boltzmann scaling. Connectivity can accelerate the wetting front along preferential flow paths, leading to anomalous super-diffusion. In other soils, organized regions of low permeability can retard flow, causing anomalous sub-diffusion. Fractal models are useful to describe soil heterogeneity (see the review by Xu et al. [16]). Indicators of fractal-type soils include power-law distributions of pore space, particle size, and mass distribution. Tyler and Wheatcraft (1990) explain how fractal porous media can lead to anomalous diffusion. Cushman et al. [3] suggest a fractal ruler in time (i.e., a fractal clock)

$$\tau = t^\alpha, \tag{5}$$

to efficiently model this anomalous diffusion, without resorting to fractional derivatives.

Applying a fractal ruler in time yields the fractal derivative [2]

$$\frac{\partial \theta}{\partial t^\alpha} = \lim_{\Delta t \rightarrow 0} \frac{\theta(t) - \theta(t - \Delta t)}{t^\alpha - (t - \Delta t)^\alpha}. \tag{6}$$

Using this fractal derivative, consider the fractal Richards’ equation (FRE)

$$\frac{\partial \theta}{\partial t^\alpha} = \frac{\partial}{\partial x} \left[D_x(\theta) \frac{\partial \theta}{\partial x} \right], \tag{7}$$

where $D_x(\theta)$ ($L^2 T^{-\alpha}$) is a fractal water diffusivity. The FRE exhibits non-Boltzmann scaling, illustrated in Fig. 1(b). Natural soils can exhibit fractal properties [15], leading to the non-Boltzmann scaling in flow dynamics. Model (7) applies a fractal time ruler to account for the influence of soil heterogeneity on the motion of water. The fractional time derivative in Eq. (4) can be related to a random time change [10]. The FRE uses a simpler deterministic time change $\theta(\tau)$, which relates to the fractal properties of the porous medium [2,17].

Use definition (6) to verify the fractal chain rule

$$\frac{\partial \theta}{\partial t^\alpha} = \frac{\partial \theta}{\partial \lambda} \frac{\partial \lambda}{\partial t^\alpha}. \tag{8}$$

Substitute $\lambda = xt^{-\alpha/2}$ into the FRE (7), and apply Eq. (8) to obtain the ODE

$$-\frac{\lambda}{2} \frac{\partial \theta}{\partial \lambda} = \frac{\partial}{\partial \lambda} \left[D_x(\theta) \frac{\partial \theta}{\partial \lambda} \right]. \tag{9}$$

with non-Boltzmann scaling. So long as $D_x(\theta)$ does not depend on t , the non-Boltzmann scaling in Eq. (9) pertains for any functional form of the diffusivity $D_x(\theta)$.

Parlange et al. [13] proposed two basic diffusivity forms: exponential and power-law. Combining their solutions with the time change in Eq. (5) yields explicit results for the FRE (7). The exponential form assumes $D_x(\theta) = C_0 e^{n\theta}$ ($n > 0$) in a semi-infinite domain, with the initial condition $\theta(t = 0, x) = 0$ and the boundary condition $\theta(t, x = 0) = 1.0$ at the inlet. The approximate solution to Eq. (7) under these conditions is achieved by solving the following equation

$$2C_0[E_i(n) - E_i(n\theta)] = Sxt^{-\alpha/2} + \frac{A}{2}(xt^{-\alpha/2})^2, \tag{10}$$

where $E_i(x) = -\int_{-\infty}^x t^{-1} e^{-t} dt$, $S^2 = C_0[e^n(2n^{-1} - n^{-2}) - n^{-1} + n^{-2}]$, and $A = (e^n n^{-1} - 1 - n^{-1})/(e^n - 1)$. The approximate solution of (7) with a power-law diffusivity $D_x(\theta) = C_0 \theta^n$ ($n > 0$) is then given by

$$\theta^n = 1 - \frac{n}{2C_0} \left[\sqrt{\frac{2C_0(1-g/2)}{n+1}} xt^{-\alpha/2} + \frac{g}{2} (xt^{-\alpha/2})^2 \right], \tag{11}$$

where $g = 1 - (2\sqrt{(n+1)/n} - 1)^{-1}$. The normalized water content curves predicted by FRE (7) with exponential and power-law diffusivities are presented in Fig. 2. Detailed comparison with numerical solutions (see discussion) indicate that the approximate analytical solutions are reasonably accurate for a wide range of n .

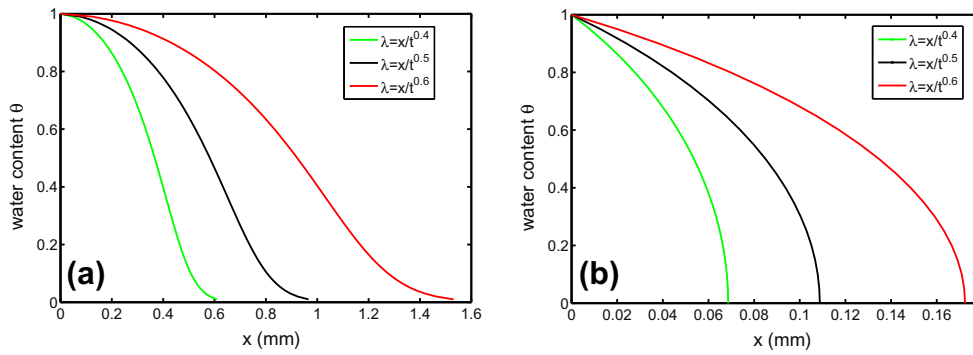


Fig. 2. Normalized water content described by the FRE (7) at time $t = 100$ with the exponential diffusivity $D_x(\theta) = C_0 e^{n\theta}$ (a), and the power-law diffusivity $D_x(\theta) = C_0 \theta^n$ (b) with $C_0 = 10^{-4}$ and $n = 2.0$.

3. Applications

Fig. 3 illustrates the results of fitting the FRE (7) with a power-law diffusivity to water content data in both fired-clay brick and siliceous brick, measured by El Abd and Milczarek [4]. The solid lines show the FRE fit, and the dotted lines show best-fit solutions using the classical Richards' Eq. (1). Model parameters, including the non-Boltzmann scaling exponent α , were fitted using the first two groups of water content data (at time $t = 419$ s and 2219 s, respectively), and the remaining three curves at later times were then predicted using the same model parameters. In Fig. 3(b), the results from fractional Richards' Eq. (4) are also included. The fractional Richards' equation is not applicable in the super-diffusive case of Fig. 3(a), since it is limited to $\alpha/2 < 1/2$.

Fig. 3 shows two data sets from experiments reported in El Abd and Milczarek [4], and fitted wetting fronts from the relevant models. Solid lines represent the fractal Richards' Eq. (7) developed in this paper, dotted lines show the traditional Richards' Eq. (1), and the dashed lines in Fig. 3(b) indicate the fractional Richards' Eq. (4). Since the traditional Richards' equation follows Boltzmann scaling, it under-estimates the wetting fronts for super-diffusion (Fig. 3(a)), and over-estimates the wetting fronts for sub-diffusion (Fig. 3(b)). Fig. 3 indicates that the fractal model (7) fits the wetting front more closely (the mean squared error, or $MSE = 0.005$) than the classical Richards' Eq. (1) ($MSE = 0.114$), especially at later times. These mean squared error values were computed by pooling data from all curves shown. The data resolution reported in El Abd

and Milczarek [4] was 0.2 mm, and taking this into account, the MSE could vary by at most 0.01. Hence the fractal model provides an improved fit. The fractional Richards' Eq. (4) is not applicable to this super-diffusive data set, since it is limited to the sub-diffusive regime $\alpha/2 < 1/2$.

The alternative fractional Richards' Eq. (4) gives an improved fit (dashed lines in Fig. 3(b)) as compared to the traditional Richards' equation (dotted lines), since it captures the sub-diffusive effect. The fractal model (solid lines) seems to provide some marginal improvement at later times ($t = 79770$ s and 170430 s). For Fig. 3(b), we find $MSE = 0.1229$ for the classical Richards' equation, $MSE = 0.0376$ for the fractional Richards' equation, and $MSE = 0.0357$ for the fractal Richards' equation developed in this paper.

Even though the brick materials used in the experiments of El Abd and Milczarek [4] are quite homogeneous, significant anomalous diffusion is evident in the wetting fronts. This indicates that even a small degree of heterogeneity can have a measurable effect on diffusion, which should be accounted for in practical applications.

4. Discussion

The FRE model (7) with constant coefficients captures non-Boltzmann scaling. It can be related to the traditional Richards' equation with a time-dependent diffusivity. Guerrini and Swartzendruber [7] and Abd El-Ghany El-Abd and Milczarek [4] write $D(\theta, t) = E(\theta)t^m$, where E is a function of water content. The parameter $m = \alpha - 1$ leads to non-Boltzmann scaling $x = \lambda(\theta)t^{2/2}$. The

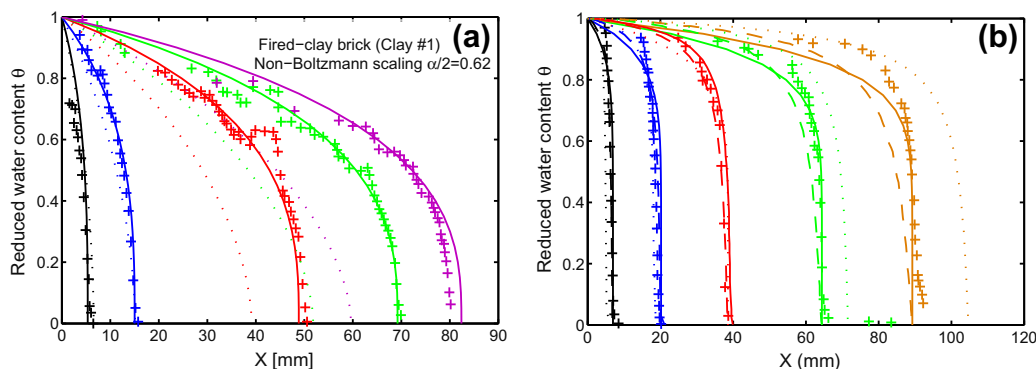


Fig. 3. Application of classical, fractional and fractal Richards' equations to experimental data from [4]. The dotted, dashed (right panel only), and solid lines represent solutions to the best-fitting classical, fractional and fractal Richards' equations, respectively. (a) Experimental wetting front data in a fired-clay brick, with fitted classical and fractal Richards' equation models, using a power-law diffusivity $D_x(\theta) = C_0 \theta^n$ (mm^2/s^2). The corresponding times for five groups of data are $t = 419$ s, 2219 s, 14879 s, 26099 s and 34559 s, respectively. Best-fit parameters for the classical model are $C_0 = 0.075$ and $n = 1.75$. In the FRE (7), best-fit parameters are $C_0 = 0.02$ and $n = 2.85$. (b) Experimental data for a siliceous brick, and fitted classical, fractional and fractal Richards' equation solutions. The corresponding times for five groups of data are $t = 450$ s, 5370 s, 24,210 s, 79,770 s and 170,430 s, respectively. The solution curves for FRE (7) were obtained using the power-law diffusivity $D_x(\theta) = C_0 \theta^n$ (mm^2/s^2) with best-fit parameters $C_0 = 0.98$ and $n = 8.2$. The water content curves for the classical and fractional Richards' equations are reproduced from Fig. 9 in [6].

term $t^m = t^{\alpha-1}$ in the diffusivity function can be absorbed into the time derivative, leading to a constant coefficient model with

$$t^{1-\alpha} \frac{\partial \theta}{\partial t} = \alpha \frac{\partial \theta}{\partial t} \frac{\partial t}{\partial t^\alpha} = \alpha \frac{\partial \theta}{\partial t^\alpha}. \quad (12)$$

The FRE (7) can be solved using an implicit Adams–Bashforth–Moulton scheme

$$\frac{\theta_i^j - \theta_i^{j-1}}{t_j^\alpha - t_{j-1}^\alpha} \Delta x = \frac{1}{2} \left[(D(\theta_{i+1}^j) + D(\theta_i^j)) \frac{\theta_{i+1}^j - \theta_i^j}{\Delta x} - (D(\theta_i^j) + D(\theta_{i-1}^j)) \frac{\theta_i^j - \theta_{i-1}^j}{\Delta x} \right], \quad (13)$$

where θ_i^j denotes the water content at location $x = i\Delta x$ and time $t = j\Delta t$. This numerical method was implemented, and used to validate the analytical approximations in Eqs. (10) and (11). For example, the relative error in Eq. (10) for the case $\alpha = 0.8$, $C_0 = 0.02$, and $n = 2$ at $\theta = 0.1$ is less than 0.5%. For vertical water infiltration in an unsaturated medium, the influence of gravity usually should be considered. The corresponding fractal Richards' equation can be written as

$$\frac{\partial \theta}{\partial t^\alpha} = \frac{\partial}{\partial x} \left[D_x(\theta) \frac{\partial \theta}{\partial x} - K_x \right], \quad (14)$$

where K_x is the hydraulic conductivity. The same numerical method can also be used to solve Eq. (14).

The fractal-time concept may be useful to extend other models of unsaturated flow in heterogeneous porous media. For example, the stochastic models for unsaturated flow developed by Harter and Yeh [8] and Amir and Neuman [1] might be modified in this way to capture observed anomalous behavior.

The wetting front in fired-clay brick (Fig. 3(a)) moves faster than in siliceous brick (Fig. 3(b)). The firing process could evaporate air bubbles, increasing the effective pore space. The FRE, with a simple power-law diffusivity, captures both anomalous motions, where the exponent $\alpha/2$ in non-Boltzmann scaling can be either larger than 0.5 (super-diffusion) or less than 0.5 (sub-diffusion). Table 1 illustrates that the value of $\alpha/2$ is higher in limestone than in silty clay. The physical mechanisms that cause non-Boltzmann scaling are not known. While the brick materials used in by El Abd and Milczarek [4] are relatively homogeneous, it is not possible to manufacture a perfectly homogeneous material. Hence fractal models of porous media might provide one explanation. Further research is needed to explore the connection between the fractal time index α and soil texture parameters, including the fractal dimension.

5. Conclusion

A simple extension of Richards' equation was proposed to model non-Boltzmann scaling of wetting front dynamics in unsaturated porous media. The FRE (7) uses a power-law clock in time to capture anomalous non-Boltzmann scaling. By varying the fractal time index $0 < \alpha < 2$, the full range of observed behavior can be represented. This includes the sub-diffusive regime, when regions of low permeability can retard flow, and super-diffusion, where the wetting front is accelerated along preferential flow paths. The fractal clock may relate to a well-established fractal model for soils.

Numerical solutions and simple analytical approximations are presented for the model. Two applications are presented, to show that the fractal Richards' equation can predict wetting front dynamics for both sub-diffusive and super-diffusive examples in a laboratory setting. The fractal clock employed by this study could be applied in other settings, to capture anomalous diffusion in heterogeneous porous media.

Acknowledgment

The work was supported by the USA National Science Foundation under DMS-0803360, DMS-1025417 and DMS-1025486. H.S. was also supported by the Natural Science Foundation of China under 11202066, National Basic Research Program of China (973 Project No. 2010CB832702) and the R&D Special Fund for Public Welfare Industry (Hydrodynamics, Project No. 201101014). J.Z. was partially supported by the Maki chair program at Desert Research Institute. M.M.M. was partially supported by the USA National Institutes of Health, grant R01-EB012079. We also thank Scott W. Tyler and three anonymous reviewers for suggestions that significantly improved the presentation of this work.

References

- [1] Amir O, Neuman SP. Gaussian closure of one-dimensional unsaturated flow in randomly heterogeneous soils. *Water Resour Res* 2001;44(2):355–83.
- [2] Chen W. Time-space fabric underlying anomalous diffusion. *Chaos Soliton Fract* 2006;28: 923–9.
- [3] Cushman JH, O'Malley D, Park M. Anomalous diffusion as modeled by a nonstationary extension of Brownian motion. *Phys Rev E* 2009;79:032101.
- [4] Abd El-Ghany El-Abd, Milczarek JJ. Neutron radiography study of water absorption in porous building materials: anomalous diffusion analysis. *J Phys D: Appl Phys* 2004;37:2305–13.
- [5] Ferguson H, Gardner WH. Diffusion theory applied to water flow data obtained using gamma ray absorption. *Soil Sci Soc Am Proc* 1963;27(3): 243–6.
- [6] Gerolymatou E, Vardoulakis I, Hilfer R. Modelling infiltration by means of a nonlinear fractional diffusion model. *J Phys D: Appl Phys* 2006;39: 4104–10.
- [7] Guerrini IA, Swartzendruber D. Soil water diffusivity as explicitly dependent on both time and water content. *Soil Sci Soc Am J* 1992;56:335–40.
- [8] Harter T, Yeh TCJ. Flow in unsaturated random porous media, nonlinear numerical analysis and comparison to analytical stochastic models. *Water Resour Res* 1998;22(3):257–72.
- [9] Küntz M, Lavallée P. Experimental evidence and theoretical analysis of anomalous diffusion during water infiltration in porous building materials. *J Phys D: Appl Phys* 2001;34:2547–54.
- [10] Meerschaert MM, Scheffler H-P. Limit theorems for continuous time random walks with infinite mean waiting times. *J Appl Prob* 2004;41:623–38.
- [11] Meerschaert MM, Sikorskii A. *Stochastic Models for Fractional Calculus*. Berlin: De Gruyter; 2012.
- [12] Pachepsky Y, Timlin D, Rawls W. Generalized Richards' equation to simulate water transport in unsaturated soils. *J Hydrol* 2003;272:3–13.
- [13] Parlange MB, Prasad SN, parlange JY, Romkens MJM. Extension of the Heaslet-Alksne technique to arbitrary soil water diffusivities. *Water Resour Res* 1992;28(10):2793–7.
- [14] Richards LA. Capillary conduction of liquids through porous mediums. *Physics* 1931;1:318–33.
- [15] Tyler SW, Wheatcraft SW. Fractal processes in soil-water retention. *Water Resour Res* 1990;26(5):1047–54.
- [16] Xu TB, Moore ID, Gallant JC. Fractals, fractal dimensions and landscapes—a review. *Geomorphology* 1993;8:245–62.
- [17] Wheatcraft SW, Tyler SW. An explanation of scale-dependent dispersivity in heterogeneous aquifers using concepts of fractal geometry. *Water Resour Res* 1988;24(4):566–78.